Physics in Medicine & Biology

PAPER

Preclinical voxel-based dosimetry through GATE Monte Carlo simulation using PET/CT imaging of mice

To cite this article: Arun Gupta *et al* 2019 *Phys. Med. Biol.* **64** 095007

IOP Publishing Phys. Med. Biol. 64 (2019) 095007 (11pp) https://doi.org/10.1088/1361-6560/ab134b

Physics in Medicine & Biology

IPEM Institute of Physics and Engineering in Medicine

PAPER

Preclinical voxel-based dosimetry through GATE Monte Carlo simulation using PET/CT imaging of mice

RECEIVED
24 July 2018

REVISED
3 March 2019

ACCEPTED FOR PUBLICATION
26 March 2019

PUBLISHED
26 April 2019

Arun Gupta[1], **Min Sun Lee**[1,2], **Joong Hyun Kim**[3], **Sohyeon Park**[4], **Hyun Soo Park**[4], **Sang Eun Kim**[4], **Dong Soo Lee**[1] and **Jae Sung Lee**[1,2,5,6,7]

[1] Department of Nuclear Medicine, College of Medicine, Seoul National University, Seoul, Republic of Korea
[2] Interdisciplinary Program in Radiation Applied Life Science, Seoul National University, Seoul, Republic of Korea
[3] Center for Ionizing Radiation, Korea Research Institute of Standards and Science, Daejeon, Republic of Korea
[4] Department of Transdisciplinary Studies, Graduate School of Convergence Science and Technology, Seoul National University, Suwon, Republic of Korea
[5] Department of Biomedical Sciences, College of Medicine, Seoul National University, Seoul, Republic of Korea
[6] Department of Nuclear Medicine, Seoul National University College of Medicine, 103 Daehak-ro, Jongno-gu, Seoul 03080, Republic of Korea
[7] Author to whom any correspondence should be addressed.

E-mail: jaes@snu.ac.kr

Keywords: preclinical, PET/CT, voxel-based dosimetry, GATE Monte Carlo, MIRD

Abstract

Internal dosimetry is of critical importance to obtain an accurate absorbed dose-response relationship during preclinical molecular imaging and targeted radionuclide therapy (TRT). Conventionally, absorbed dose calculations have been performed using organ-level dosimetry based on the Medical Internal Radiation Dose (MIRD) schema. However, recent research has focused on developing more accurate voxel-level calculation methods. Geant4 application for emission tomography (GATE) Monte Carlo (MC) is a simulation toolkit gaining attention in voxel-based dosimetry. In this study, we used PET/CT images of real mice to estimate the absorbed doses in sensitive organs at voxel-level to evaluate the suitability of GATE MC simulation for preclinical dosimetry. Thirteen normal C57BL/6 mice (male, body weight: 27.71 $\pm$ 4.25 g) were used to acquire dynamic positron emission tomography/computed tomography (PET/CT) images after IV injection of ^{18}F-FDG. GATE MC toolkit was applied to estimate the absorbed doses in various organs of mice at voxel-level using CT and PET images as voxelized phantom and voxelized source, respectively. In addition, mean absorbed dose at organ-level was calculated using MIRD schema for comparison purposes. The differences in the respective absorbed doses (mGy MBq^{-1}) between GATE MC and MIRD schema for brain, heart wall, liver, lungs, stomach wall, spleen, kidneys, and bladder wall were 1.36, 12.3, −22.4, −11.2, −16.9, −2.87, −4.29, and 3.71%, respectively. Considering that the PET/CT data of real mice were used for GATE simulation, the absorbed doses estimated in this study are mouse-specific. Therefore, the GATE-based Monte Carlo is likely to allow for more accurate internal dosimetry calculations. This method can be used in TRT for personalized dosimetry because it considers patient-specific heterogeneous tissue compositions and activity distributions.

1. Introduction

Internal dosimetry is of critical importance for an effective analysis of the risk-benefits of the nuclear medicine imaging and targeted radionuclide therapy (TRT) (Sarrut *et al* 2014). With the increasing use of newer radiopharmaceuticals in targeted imaging and therapy, accuracy of absorbed dose-response relationship is becoming a critical factor in preclinical dosimetry as well (Kostou *et al* 2016). Absorbed dose in small animals can be estimated using the methods recommended by the Medical Internal Radiation Dose (MIRD) committee (Kolbert *et al* 2003, Funk *et al* 2004, Boutaleb *et al* 2009). MIRD is a generalized formalism for estimation of absorbed dose, and it is traditionally applied at the organ-level using *S*-values (mean absorbed dose in a target organ per radioactivity decay in a source organ) also known as dose factors released by the radiation dose assessment resource

(RADAR) group (Loevinger *et al* 1988, Stabin and Siegel 2003, Mauxion *et al* 2013). Nevertheless, this approach assumes homogeneous activity and dose distributions in organs and a generalized geometry; hence, it does not incorporate patient- or animal-specific activity distributions and organ anatomies (Hippelainen *et al* 2015, Lee *et al* 2018). Furthermore, absorbed dose in an organ or a tumor, during radionuclide therapy, can be estimated using a software, named OLINDA, (Stabin *et al* 2005) that uses the RADAR formalism of dose calculation and assumes a spherical tumor geometry. However, the geometry is not robust enough to model the size, shape, and location of every unique tumor in the reference phantoms used in OLINDA (Parach *et al* 2011).

The limitations of the organ-level MIRD method have been addressed by several researchers, and various steps have been taken to extend the MIRD formalism to voxel-based dosimetry using voxel *S*-values (Muthuswamy *et al* 1998, Bolch *et al* 1999, 2009, Flynn *et al* 2001). However, a database of preclinical voxel *S*-values of different radionuclides at several voxel dimensions is not yet available to perform voxel-based dosimetry in small animals using MIRD schema. Therefore, voxel-based dosimetry using direct Monte Carlo (MC) approach is considered a potentially more accurate method because it considers heterogeneity within the mouse body in respect of both activity distributions and tissue compositions (Hui *et al* 1994, Dewaraja *et al* 2005, Sgouros *et al* 2008, Boutaleb *et al* 2009). Specific absorbed fractions (SAFs) and organ-level *S*-values of murine models for different PET and SPECT radionuclides have been estimated from realistic digital phantoms of whole-body mouse (MOBY) and rat (ROBY) using MC simulation codes such as MCNP, EGSnrc, GATE/Geant4, etc (Segars *et al* 2004, Stabin *et al* 2006, Bitar *et al* 2007, Larsson *et al* 2007, Keenan *et al* 2010). Xie and Zaidi (2013) generated a database of *S*-values for the assessment of radiation dose to mice from different PET radionuclides using MOBY phantoms and MCNPX MC code.

Recently, the Geant4 application for emission tomography (GATE) MC simulation platform (Jan *et al* 2004) based on the Geant4 toolkit (Agostinelli *et al* 2003) has gained importance in voxel-based dosimetry. Although the GATE has been widely validated, there are very limited studies reporting its application in preclinical dosimetry (Taschereau and Chatziioannou 2007, Mauxion *et al* 2013, Perrot *et al* 2014, Kostou *et al* 2016). Taschereau and Chatziioannou (2007) calculated absorbed dose distributions from ^{18}F-FDG PET imaging of mice using GATE MC and MOBY phantoms. Mauxion *et al* (2013) performed a study with MCNPX and GATE MC codes to assess the impact of organ mass on absorbed dose from ^{18}F-FDG using MOBY phantoms. Parach *et al* (2011) calculated organ doses from the digital geometry of a Snyder mathematical phantom using GATE MC and compared the results with the MIRD data previously published by Snyder *et al* (1969). This comparison is meaningful because GATE is the only open access MC code dedicated for nuclear medicine dosimetry and MIRD is the most widely accepted system for internal dosimetry in nuclear medicine.

Most recently, Kostou *et al* (2016) used GATE simulation and the MOBY phantom to calculate the *S*-values of commonly used radioisotopes including ^{18}F with whole-body heterogeneous activity distributions as the source organ. Moreover, they performed the studies using the MOBY phantom developed by Segars *et al* (2004) which is based on non-uniform rational B-spline (NURBS) mathematical models. Since even a small variation in anatomy can significantly impact the dose calculations, it is not possible to create a specific mouse model with standardized organs and anatomy to implement personalized dosimetry for murine studies (Boutaleb *et al* 2009, Kostou *et al* 2016). Therefore, dosimetry simulations using PET/CT imaging data of individual mice might preclude the dose estimation errors arising from the variations in organ anatomies and activity distributions.

In this study, we calculated absorbed dose in normal mice at voxel-level using the most commonly used PET radiotracer, ^{18}F-fluorodeoxyglucose (^{18}F-FDG) to evaluate the feasibility of GATE MC toolkit for reliable use in preclinical voxel-based dosimetry. More importantly, we applied the CT and PET images of real mice for GATE MC simulations instead of a MOBY phantom. We also performed an image-based dosimetry at the organ-level using MIRD schema to compare with the voxel-based absorbed dose obtained with GATE MC simulation. In addition, we analyzed the dose absorbed in the urinary bladder wall because kidneys are the main excretory organs for ^{18}F-FDG, which remains unvoided for a long duration during dynamic PET imaging.

2. Materials and methods

2.1. Animal

All the animal studies were approved by the Institutional Animal Care and Use Committee (IACUC) of Seoul National University Bundang Hospital (SNUBH), Seongnam, Korea (IACUC No. BA1708-229/072-01). Thirteen normal male mice (C57BL/6) of 10–12 weeks old, each weighing 27.71 $\pm$ 4.25 g, were used in this study. The mice were kept in a specific pathogen-free room maintained at ~21 °C and ~55% RH on a 12 h light/dark cycle, with food and water available ad libitum. The mice were fasted overnight for ^{18}F-FDG PET/CT imaging.

2.2. Preclinical PET/CT imaging

The NanoPET/CT imaging system (Mediso Inc., Budapest, Hungary) was employed in this study. The 90 min whole-body dynamic PET imaging was initiated immediately after administering an IV injection of ^{18}F-FDG

(15.22 ± 2.49 MBq) to each mouse via a catheter inserted in its tail vein. An x-ray CT transmission scan was performed after the PET scan to correct for gamma-ray attenuation and to obtain anatomical information. The mice were maintained under 2% isoflurane anesthesia during the PET/CT scanning. All the dynamic frames were reconstructed using the iterative 3D ordered subset expectation maximization (OSEM) algorithm and single-slice rebinning (SSRB) method. Corrections were applied for attenuation, scatter, and decay during image reconstruction. Thirty-four dynamic frames (4×3 s, 6×1 s, 7×6 s, 8×30 s, 1×300 s, and 8×600 s) were generated from the 90 min list-mode PET data. The reconstructed images had a dimension of $80\times80\times223$ with a 0.60 mm transaxial spacing and a 0.60 mm axial slice interval. A calibration factor was measured from uniform syringe phantoms (5 cm^3) filled with ^{18}F-FDG to correct for the activity concentration (Bq ml^{-1}) on the reconstructed PET images of mice.

2.3. Image analysis and organ mass estimation

The reconstructed dynamic PET frames were summed to a 90 min time-integrated PET image (i.e. activity images representing the total duration of the study) using MATLAB. The volumes of interest (VOIs) were manually drawn over the major organs (brain, heart, lungs, liver, stomach, spleen, kidneys, and urinary bladder) on the CT and 90 min time-integrated PET images using MRIcro tool as shown in figures 1(a) and (b). We used the fused PET and CT images as reference while drawing VOIs like the heart wall, stomach wall, and bladder wall. Care was taken to ensure that the regions were not overlapped while drawing a VOI. The number of voxels in each organ was calculated and then multiplied by the voxel volume and tissue density to estimate its organ mass. The tissue densities used in this study were taken from the International Commission on Radiological Protection (Valentin 2002). The estimated organ mass was used for the mass correction while using the *S*-values published by Xie and Zaidi (2013) for organ-level dosimetry.

2.4. PET image-based biodistribution of ^{18}F-FDG

The ^{18}F-FDG uptakes in different organs were estimated for each mouse by applying VOIs over the respective organs on the reconstructed PET images. Figures 1(c)–(h) show the VOIs superimposed on the PET frames at different post-injection time points. The PET image-based biodistribution data obtained from the organs were plotted as a function of time to generate time activity curves (TACs). The activity measured in an organ (MBq) was normalized to the total injected activity to express the injected activity in percentage (%IA). The time-integrated activity ($\widetilde{A}$) in each organ was obtained by calculating the area under curve (AUC) of the respective TAC. The AUC was calculated as the trapezoidal sum of the observed data over the range of 0–90 min and extrapolated to infinity using the integral of physical decay for the curve tail at the end of the scan. Thus, the $\widetilde{A}$ was calculated as $\widetilde{A}=\int_0^\infty A\ (t)\ dt\ =\int_0^\infty A_0\exp\left(-\frac{\ln(2)}{T_{1/2}}t\right)\ dt$, where $A\ (t)$ is the activity of an organ at time t.

2.5. GATE Monte Carlo simulation setup

All simulations in this study used GATE v.7.0 which has been extended for dosimetry applications. GATE is based on the Geant4 toolkit (Agostinelli *et al* 2003) which is a well-established code for radiation transport. GATE v.7.0 utilizes Geant4 v. 9.6.3. The CT and PET images of the mice were resampled for the same voxel dimensions (0.60 mm × 0.60 mm × 0.60 mm) and used as voxelized phantom and voxelized source, the respective inputs to GATE for dosimetry simulation. The ImageRegularParametrisedVolume option was used for the simulation of voxelized phantom using the CT image of real mouse. The ^{18}F ion-source type of Geant4 v. 9.6.3 was used for the simulation. The standard electromagnetic physics package of GATE, which includes photoelectric effect, Compton, bremsstrahlung, and positron–electron annihilation, was used during all simulations. Neither an energy cut nor a variance reduction technique was applied in the physical processes. The GATE was run with Mersenne Twister (Matsumoto and Nishimura 1998) random number generator. The simulation was conducted in an in-house computing cluster with a 60-core CPU and an 80 GB RAM. For each PET frame, a separate simulation was run with the corresponding biodistribution data and PET frame durations. To reduce the simulation time and computational cost, the simulation was performed for one-tenth to one-hundredth of the acquisition time of each PET frame. However, the statistical uncertainties were kept below 2% at the voxel-level. The total time required to perform the simulations for each mouse was 894 h.

2.6. Voxel-based dosimetry using GATE MC

GATE MC simulations was used for voxel-based absorbed dose calculations. GATE contains a mechanism, named DoseActor, which stores the absorbed dose in a given volume in a 3D matrix (Sarrut *et al* 2014). The simulation outputs the energy deposition (Edep) map, dose distribution map, number of hits, and local statistical uncertainty. By using the DoseActor mechanism, deposited energy [*J*] in the voxels within the VOIs drawn over each organ was estimated from all thirty-four Edep maps. Subsequently, the absorbed dose in the voxels were calculated by dividing the deposited energy in each voxel with the voxel mass. Finally, the voxel doses within the VOIs were summed to obtain the organ absorbed dose. We then calculated dose rate (Gy s^{-1}) in each organ from

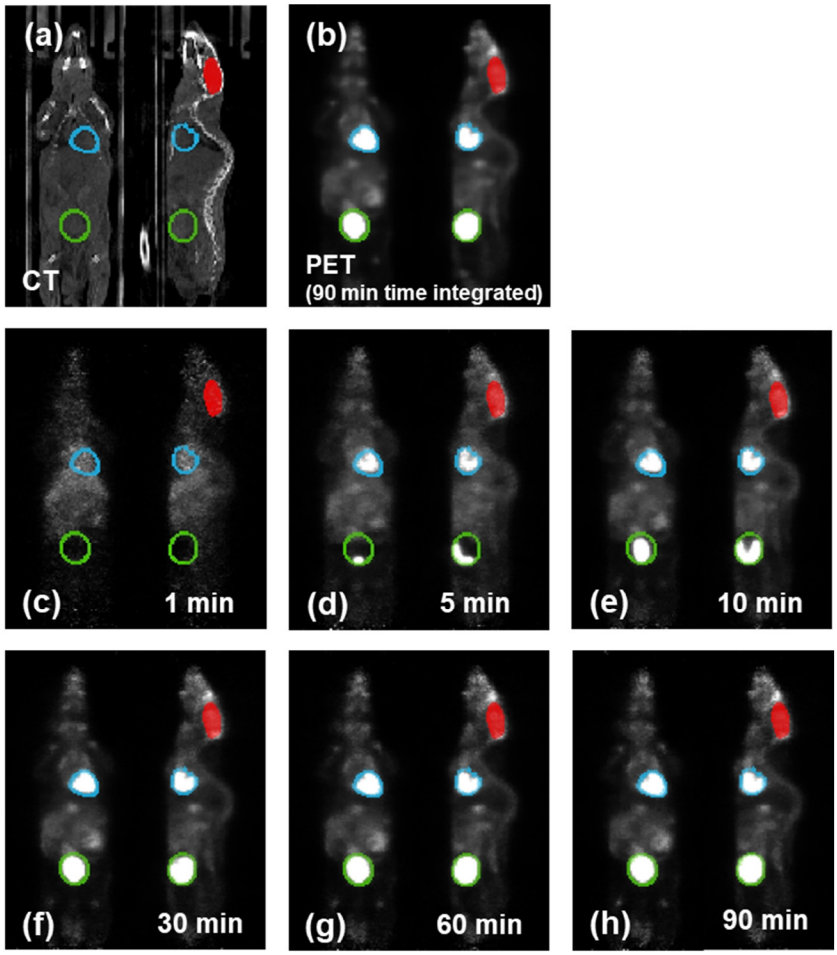

Figure 1. VOIs drawn on brain, heart wall, and bladder wall on CT image (a) and 90 min time-integrated PET image (b). VOIs are superimposed on selected PET frames (c)–(h) at different time points post-injection. Coronal (left) and sagittal (right) views of CT and PET images, respectively, are shown.

the PET frame by dividing the absorbed dose with the respective simulation time. The dose rate versus time curves were plotted to measure the total absorbed dose in each organ using AUCs. The AUC of each dose-rate curve was calculated as the trapezoidal sum of the observed data over the range of 0–90 min and extrapolated to infinity using the integral of physical decay for the curve tail. The estimated absorbed dose at voxel-level was normalized to the injected activity of ^{18}F-FDG in each mouse and presented in mGy MBq^{-1}. The steps followed for voxel-based absorbed dose estimation using GATE MC simulation are illustrated in figure 2.

2.7. Image-based dosimetry at organ-level using MIRD schema

Based on the MIRD schema (Bolch *et al* 2009), we measured the mean absorbed dose at organ-level using the same PET/CT imaging data of mice for comparison with the results of voxel-based dosimetry estimated with GATE MC. The mean absorbed dose (D) in the target organ (r_t) was calculated using the time-integrated activity ($\widetilde{A}$) in the source organs (r_s) obtained from the PET image-based biodistribution data and the S-values ($S(r_t \leftarrow r_s)$) using the following equation:

$$D(r_t \leftarrow r_s) = \widetilde{A} \times S(r_t \leftarrow r_s). \quad (1)$$

The self- and cross-dose S-values of ^{18}F radioisotope for the source–target organ pairs were taken from the database published by Xie and Zaidi (2013) to calculate the self- and cross-absorbed dose in each organ. We would like to point out that the S-values estimated by them were based on the MOBY phantoms and MCNPX MC code. Organ mass correction was performed while using S-values of appropriate body weight of mouse. The relative differences between the absorbed dose values estimated from GATE MC and the corresponding values obtained with MIRD schema were calculated and compared.

2.8. Urinary bladder dose estimation

In this study, the absorbed dose to the bladder wall was estimated in a more realistic manner by applying both elastic and inelastic models of bladder absorbed dose calculations derived by Taschereau and Chatziioannou

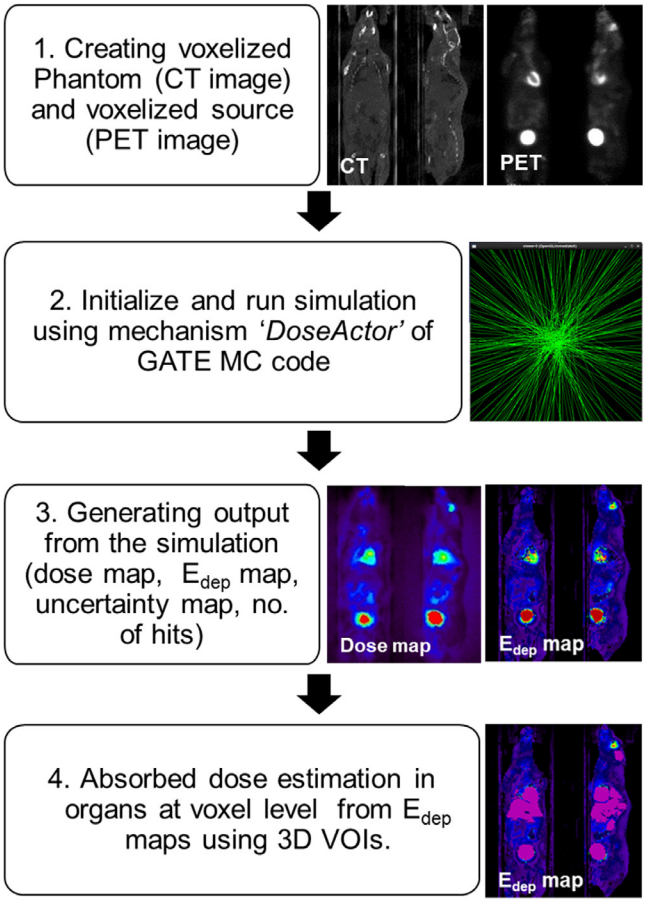

Figure 2. Methods applied to estimate absorbed dose at voxel-level using GATE MC simulation.

(2007). The voxel-based absorbed dose to bladder wall was calculated at different voiding time points after activity administration (90, 105, 120, and 135 min) with various voiding fractions (30, 50, and 80%).

3. Results

3.1. PET image-based biodistribution of ^{18}F-FDG

The TACs of eight organs are shown in figure 3. The biodistributions of ^{18}F-FDG in the organs were presented in %IA. The maximum peaks observed in the organ biodistributions were ~16% in liver (the highest uptake), followed by ~5% in heart, ~3.5% in lungs, and ~3.25% in brain. The activity uptakes in the other organs were minimal (<2%). The activity (%IA) was observed to decrease with time except for heart and bladder. Kidneys are the main excretory organs for ^{18}F-FDG, and hence the activity in the bladder increased rapidly with time, which was measured to be more than 25% of the total injected activity.

3.2. Energy deposition maps and 3D dose rate

The energy deposition maps were obtained from the GATE MC simulations for each PET frame. The energy deposited in an organ as shown in the Edep map (figure 4(b)) was observed to be similar with the ^{18}F-FDG accumulation in that organ on the PET image (figure 4(a)). The Edep map overlaid on the CT image (figure 4(c)) shows that the deposited energy was maximum in the bladder wall followed by heart wall, kidneys, and brain. The graphs of 3D dose rate versus time of eight organs (uncorrected for radiation decay) are shown in figure 5.

3.3. Voxel-based absorbed dose estimation by GATE MC simulation

Table 1 shows the mean and standard deviation (thirteen mice) of the voxel-based absorbed dose in the major organs (brain, heart wall, lungs, liver, stomach wall, spleen, kidneys, and bladder wall) estimated by GATE MC simulation, where the absorbed doses are normalized to the administered activity (mGy MBq^{-1}). The urinary bladder wall exhibited the highest absorbed dose (175 $\pm$ 61.3 mGy MBq^{-1}) followed by heart wall (48.1 $\pm$ 31.0 mGy MBq^{-1}), kidneys (39.4 $\pm$ 15.3 mGy MBq^{-1}), lungs (36.3 $\pm$ 18.1 mGy MBq^{-1}), and brain (24.3 $\pm$ 7.28 mGy MBq^{-1}). The absorbed doses in the remaining organs were less than 21 mGy MBq^{-1}. The variation in the absorbed dose for the same organ was attributed to the variations in the organ anatomy and

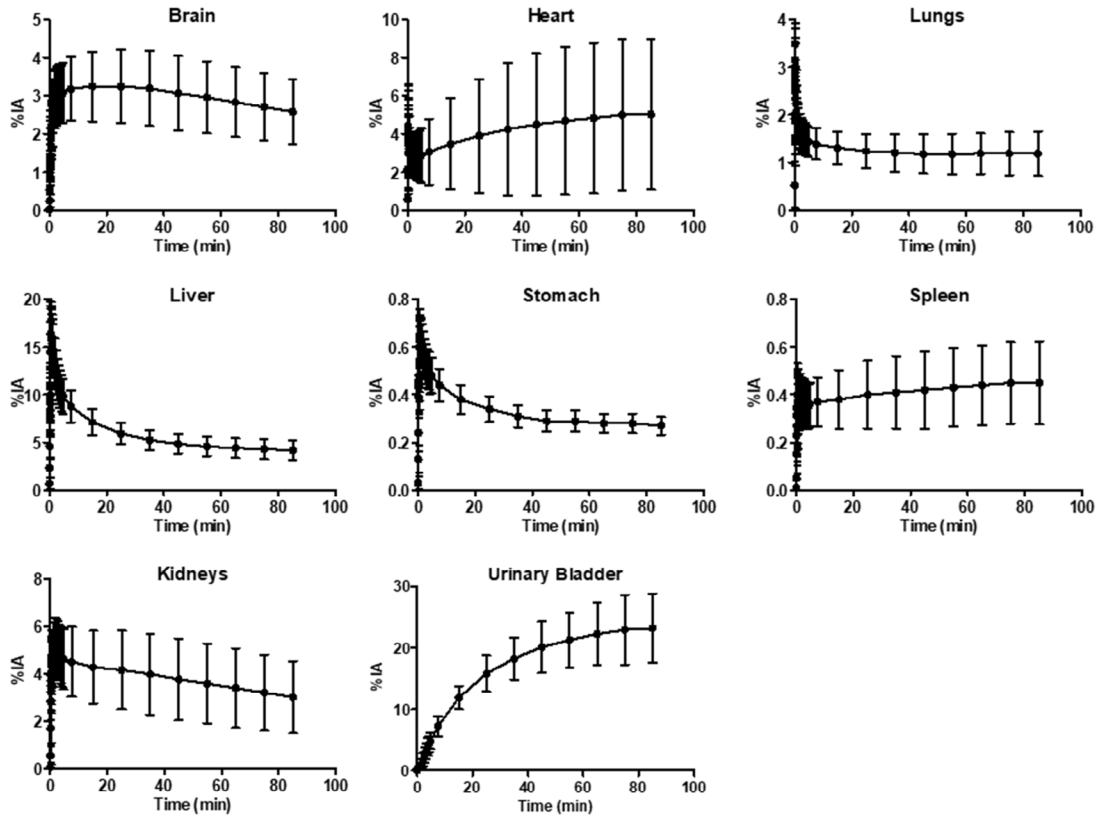

Figure 3. Graphs of percentage injected activity (%IA, mean ± SD) versus time for the eight organs (corrected for radiation decay). SD, standard deviation.

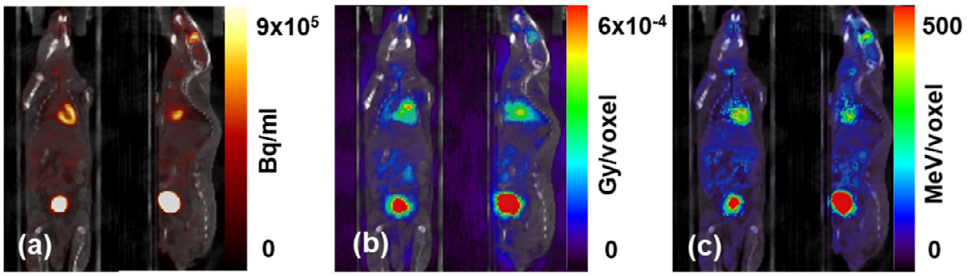

Figure 4. PET/CT fused image (a), the dosemap overlaid on CT image (b) and the Edep map overlaid on CT image (c). The left and right images in the figures represent the coronal and sagittal views, respectively.

radiotracer biodistribution among the mice. The absorbed dose estimated in each organ by GATE MC represents the sum of the self- and cross-absorbed doses.

3.4. Absorbed dose estimation at organ-level by MIRD schema

We estimated image-based organ-level mean absorbed dose for each organ using MIRD schema and normalized the value to the administered activity (mGy MBq^{-1}). The mean ± SD values of the self-absorbed, cross-absorbed, and total absorbed doses for each organ estimated using the self- and cross-absorbed *S*-values are presented in table 2.

3.5. Comparison between GATE MC and MIRD approach

The voxel-based absorbed dose estimated by GATE MC simulation was found to be comparable with the mean absorbed dose at organ-level calculated by MIRD schema for all organs except for liver and stomach wall that exhibited significant differences. The percentage differences were 1.36, 12.3, −22.4, −11.2, −16.9, −2.87, −4.29, and 3.71% for brain, heart wall, liver, lungs, stomach wall, spleen, kidneys, and bladder wall, respectively (figure 6). The overall average percentage difference in absorbed dose between these two dosimetry methods was −5.02%.

The absorbed doses calculated using GATE MC and MIRD schema in this study were compared with the similar studies performed by Taschereau and Chatziioannou (2007) and Xie and Zaidi (2013). Overall, there was

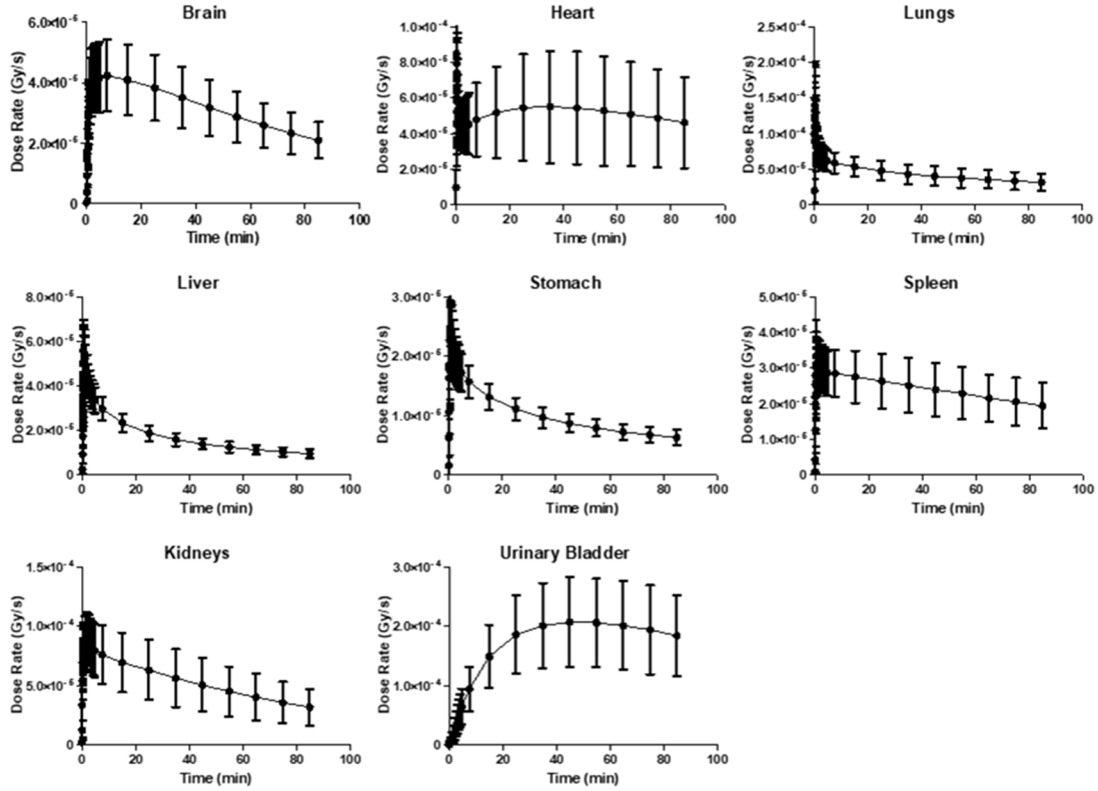

Figure 5. Graphs of 3D dose rate (mean ± SD) versus time measured from Edep maps for the eight organs (uncorrected for radiation decay). SD = standard deviation.

Table 1. Voxel-based absorbed dose in major organs (mean ± SD) estimated from ^{18}F-FDG using GATE MC simulations and normalized to the administered activity (mGy MBq^{-1}).

Organs	Voxel-based absorbed dose (mGy MBq^{-1})
Brain	24.3 ± 7.28
Heart wall	48.1 ± 31.0
Liver	11.9 ± 2.73
Lungs	36.3 ± 18.1
Stomach wall	7.29 ± 0.77
Spleen	20.6 ± 6.25
Kidneys	39.4 ± 15.3
Bladder wall	175 ± 61.3

Table 2. Mean absorbed doses (self, cross, and total) at organ-level in major organs (mean ± SD) estimated from ^{18}F-FDG using MIRD schema and normalized to administered activity (mGy MBq^{-1}).

	Absorbed dose at organ-level (mGy MBq^{-1})		
Organs	Self-absorbed dose	Cross-absorbed dose	Total absorbed dose
Brain	22.4 ± 6.98	1.52 ± 0.52	23.9 ± 7.04
Heart wall	35.3 ± 29.4	6.33 ± 1.83	41.7 ± 31.1
Liver	10.0 ± 2.16	4.44 ± 1.97	14.4 ± 3.22
Lungs	32.4 ± 10.9	5.45 ± 1.85	37.8 ± 12.3
Stomach wall	5.22 ± 0.62	3.29 ± 0.70	8.51 ± 0.93
Spleen	17.2 ± 5.52	3.64 ± 0.75	20.8 ± 5.44
Kidneys	36.1 ± 16.0	3.22 ± 0.63	39.4 ± 15.7
Bladder wall	158 ± 57.1	9.49 ± 6.06	167 ± 58.7

good agreement between this study and their studies, as shown in figure 7. The brain region was missing in the ^{18}F-FDG-PET study performed by Xie and Zaidi; however, a small value for brain as plotted in the figure referred to the cross-absorbed dose in their study, which was found to be similar to that obtained in this study (table 2).

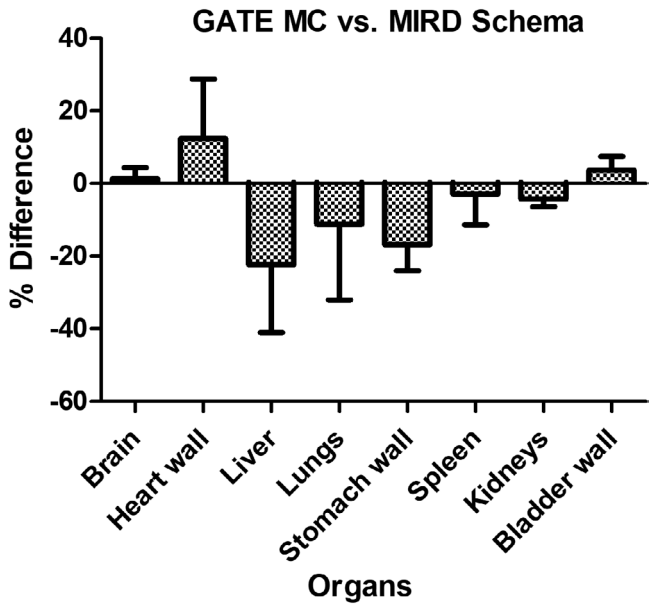

Figure 6. Percentage difference (mean ± SD) between voxel-based absorbed dose estimated by GATE MC simulation and image-based absorbed dose at organ-level estimated by MIRD schema. The positive values indicate that the absorbed dose values of GATE were larger than those of MIRD.

3.6. Urinary bladder absorbed dose

Absorbed doses to bladder wall at voxel-level calculated at different voiding time points after activity administration and various voiding fractions are summarized in table 3. It was observed that 80% voidance at $t = 90$ min could reduce the absorbed dose by 25%–30% of that measured at $t = \infty$.

4. Discussion

An accurate estimation of absorbed dose at voxel-level is a prerequisite to address the challenges of organ-level dosimetry. There have been studies on image-based dose calculations at voxel-level to provide personalized dosimetry for targeted radionuclide therapy (Kost *et al* 2015). An advantage of the Monte Carlo simulations for internal dosimetry is that they directly model the radiation transport and dose deposition within precisely defined geometries. However, there have been limited studies evaluating the reliability of GATE MC simulation in animal dosimetry. Moreover, all those studies were based on MOBY phantom. Kostou *et al* (2016) and Boutaleb *et al* (2009) concluded that there could not be a specific mouse model with standardized organs and anatomy to implement dosimetry for murine studies in general because even a small variation in mice anatomy can significantly impact the dose calculations.

In this study, we explored the feasibility of GATE MC simulation to compute the absorbed dose at voxel-level in normal mice from ^{18}F-FDG which is the most commonly used PET radiotracer in imaging procedures of both preclinical and clinical nuclear medicine. In this study, PET and CT images of real mice were used to define the voxelized activity distribution and attenuation geometry within the GATE MC simulation. This method was implemented to consider both the variations in the mouse anatomy and the actual heterogeneous radiotracer distributions for the estimation of individualized absorbed doses in each mouse. The energy deposited in each voxel was measured from the 3D energy deposition maps generated as the output of the simulations to calculate dose rate in each organ. Voxel-level absorbed dose distributions were then calculated by time-integrating the dose-rate curves. The absorbed dose in the organs correlated well with the activity biodistribution in the respective organs measured from the PET images.

The bladder wall exhibited the highest absorbed dose because of accumulation of the radiotracer in bladder. The dose was also overestimated due to the assumption that the bladder was not voided after imaging. The heart wall and brain received higher absorbed dose because of increased ^{18}F-FDG uptakes in these organs owing to high metabolic activity. Although the activity distribution and energy deposition in the lungs were small, the absorbed dose was quite high attributed to their relatively small mass and the cross-absorbed doses from heart and liver. Since the ^{18}F-FDG was excreted through renal pathways, the absorbed dose was high in kidneys.

The image-based organ-level absorbed dose was also estimated using the MIRD schema. In this method, organ anatomy and radiotracer distribution of individual mice were considered for estimation of time-integrated activity; however, the *S*-values used were calculated at organ-level and were based on MOBY phantom.

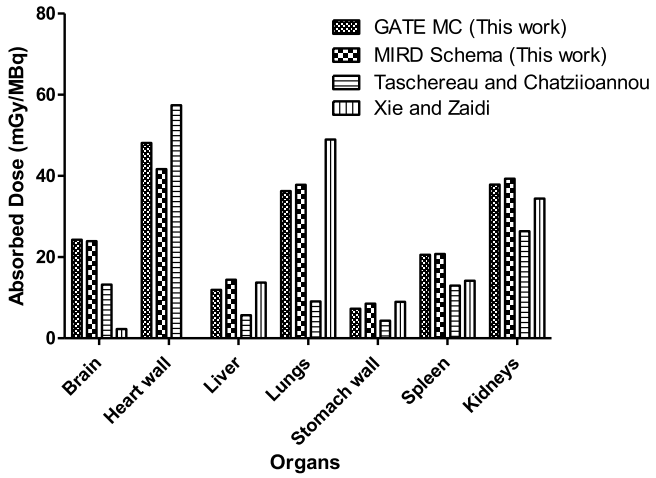

Figure 7. Comparison of absorbed doses in selected organs of mice at voxel-level (GATE MC) and organ-level (MIRD schema) calculated from ^{18}F-FDG between this study and the studies of Taschereau and Chatziioannou (2007) and Xie and Zaidi (2013).

Table 3. Absorbed dose to the bladder wall estimated by GATE MC at different voiding time points and with various voiding fractions using inelastic and elastic bladder models (Taschereau and Chatziioannou 2007).

	Inelastic model			Elastic model		
	Absorbed dose (mGy MBq^{-1}) at voiding fractions			Absorbed dose (mGy MBq^{-1}) at voiding fractions		
Post-injection voiding time (min)	30%	50%	80%	30%	50%	80%
90	155	142	122	160	150	131
	(88.8)	(81.3)	(70.1)	(92.1)	(86.2)	(75.4)
105	156	144	127	162	152	135
	(89.8)	(83.0)	(72.8)	(92.8)	(87.4)	(77.6)
120	158	147	131	163	154	139
	(90.7)	(84.5)	(75.2)	(93.4)	(88.5)	(79.6)
135	159	150	135	164	156	142
	(91.6)	(85.9)	(77.5)	(94.0)	(89.6)	(81.5)

Note: the values in the parentheses are the percentage of the absorbed dose measured at $t = \infty$.

The mean organ absorbed doses estimated by the voxel-level GATE MC simulation were comparable with those estimated using MIRD schema. The highest differences of −22% (2.50 mGy MBq^{-1}) in liver and −17% in stomach wall (1.21 mGy MBq^{-1}) were attributed to the organ *S*-values applied in MIRD schema. The differences in the size, shape, and location of the individual mouse organs as compared to the MOBY phantom organs might also be the reason for such differences in absorbed dose. In addition, the *S*-values used in this study were originally estimated for a non-labeled F-18 radioisotope; however, we used ^{18}F-FDG radiotracer for animal imaging. For different radiotracers labeled by the same radionuclide, the resulting dose distribution depends on the time-related biodistribution and may produce large discrepancies (Xie and Zaidi 2013). Parach *et al* (2011), in their study, found that the specific absorbed fraction values derived from GATE were in good agreement with the corresponding published data of MIRD.

The animal handling parameters such as dietary conditions, mode of anesthesia, and ambient temperature have a dramatic effect on ^{18}F-FDG biodistribution and therefore significantly influence the results of PET studies in mice (Fueger *et al* 2006). Taschereau and Chatziioannou (2007) estimated absorbed dose in the organs from ^{18}F-FDG at voxel-level using GATE MC simulation; however, they used MOBY phantoms for GATE simulation. The differences observed in the voxel-based absorbed doses between their study and this study were principally due to the differences in PET data analysis methods and ^{18}F-FDG biodistributions among the mouse species used. The additional discrepancies could be due to the difference in anatomy between the real mice used in this study and the MOBY phantoms used in their study. Xie and Zaidi (2013) applied MIRD schema to calculate mean organ absorbed dose using published biodistribution data of mouse and *S*-values measured from their own study. Overall, there was good agreement between this study and their study.

In this study, the absorbed dose in bladder wall at $t = 90$ min was only ~34% (59 mGy MBq^{-1}) of that estimated for infinite amount of time, $t = \infty$ (174.76 mGy MBq^{-1}). Therefore, voiding the bladder after PET

acquisition could reduce the absorbed dose significantly. The absorbed dose to bladder wall could be reduced by 25%–30% with 80% voidance at $t = 90$ min. However, the possibility of 80% voidance at 90 min is very low owing to anesthesia during imaging. It was observed in this study that the mice usually void 10–15 min after the completion of PET acquisition. Hence, if 80% voiding at $t = 105$ min was assumed, the absorbed dose to the bladder wall could be reduced by more than 20%.

GATE MC simulation is expected to yield a more realistic dose distribution in the organs at voxel-level with high accuracy because it considers the inhomogeneous activity distribution and tissue heterogeneity in the entire body. Because voxel mass can vary within an organ or a tumor due to a variation in the density of tissues within the same organ or tumor, the voxel-based absorbed dose may also vary within the organ or tumor. Furthermore, PET/CT imaging data of real mice were used in this study for dosimetry simulation, which accounts for the variations in organ anatomy and activity distribution thereby producing the individualized whole-body energy distribution for each mouse. Therefore, the voxel-based absorbed doses in the organs of mice estimated from ^{18}F-FDG PET in this study have the potential to be more accurate and mouse-specific. Additionally, the dose volume histograms (DVHs) can be generated which provide information regarding the heterogeneous distribution of absorbed dose within the target volume. This is particularly useful because it could be the starting point for a radiobiological interpretation and modeling of the dose distribution for response assessment during cancer therapy.

Although GATE MC calculations are more robust and are likely to yield more accurate internal dosimetry estimations at the voxel level, it requires extensive computational resources to reduce the simulation time, and hence it is difficult to apply in daily practice. Image-based dosimetry in mouse at voxel-level using voxel-level *S*-values of the commonly used PET and SPECT radionuclides will be performed by our team in the near future for comparison of results with direct MC voxel-based dosimetry.

5. Conclusion

We performed a detailed evaluation of GATE MC simulation for image-based radiation-absorbed dose estimation at voxel-level using ^{18}F-FDG PET/CT imaging data of normal mice. It is likely that the GATE-based Monte Carlo will allow for more accurate internal dosimetry calculations because it considers patient-specific heterogeneous tissue compositions and activity distributions. This method can be applied for personalized dosimetry in TRT to estimate maximum tolerated doses for therapy planning.

Acknowledgments

This work was supported by grants from the National Research Foundation of Korea (NRF) funded by the Korean Ministry of Science and ICT (Grant Nos. NRF-2014M3C7034000 and NRF-2016R1A2B3014645).

ORCID iDs

Jae Sung Lee https://orcid.org/0000-0001-7623-053X

References

Agostinelli S *et al* 2003 Geant4-a simulation toolkit *Nucl. Instrum. Methods Phys. Res.* A **506** 250–303

Bitar A, Lisbona A and Bardiès M 2007 *S*-factor calculations for mouse models using Monte-Carlo simulations *Q. J. Nucl. Med. Mol. Imaging* **51** 343–51 (PMID:17538523)

Bolch W E, Bouchet L G, Robertson J S, Wessels B W, Siegel J A, Howell R W, Erdi A K, Aydogan B, Costes S and Waston E E 1999 MIRD pamphlet No. 17: the dosimetry of nonuniform activity distributions-radionuclide *S* values at the voxel level *J. Nucl. Med.* **40** 11S–36S (PMID:9935083)

Bolch W E, Eckerman K F, Sgouros G and Thomas S R 2009 MIRD Pamphlet No. 21: a generalized schema for radiopharmaceutical dosimetry-standardization of nomenclature *J. Nucl. Med.* **50** 477–84

Boutaleb S, Pouget J P, Hindorf C, Pelegrin A, Barbet J, Kotzki P O and Bardies M 2009 Impact of mouse model on preclinical dosimetry in targeted radionuclide therapy *Proc. IEEE* **97** 2076–85

Dewaraja Y K, Wilderman S J, Ljungberg M, Koral K F, Zasadny K and Kaminiski M S 2005 Accurate dosimetry in ^{131}I radionuclide therapy using patient-specific, 3-dimensional methods for SPECT reconstruction and absorbed dose calculation *J. Nucl. Med.* **46** 840–9 (PMID:15872359)

Flynn A A, Green A J, Pedley R B, Boxer G M, Boden R and Begent R H J 2001 A mouse model for calculating the absorbed beta-particle dose from ^{131}I- and ^{90}Y-labeled immunoconjugates, including a method for dealing with heterogeneity in kidney and tumor *Radiat. Res.* **156** 28–35

Fueger B J, Czernin J, Hildebrandt I, Tran C, Halpern B S, Stout D, Phelps M E and Weber W A 2006 Impact of animal handling on the results of ^{18}F-FDG PET studies in mice *J. Nucl. Med.* **47** 999–1006 (PMID:16741310)

Funk T, Sun M and Hasegawa B H 2004 Radiation dose estimate in small animal SPECT and PET *Med. Phys.* **31** 2680–6

Hippeläinen E, Tenhunen M and Sohlberg A 2015 Fast voxel-level dosimetry for ^{177}Lu labelled peptide treatments *Phys. Med. Biol.* **60** 6685–700

Hui T E, Fisher D R, Kuhn J A, Williams L E, Nourigat C, Badger C C, Beatty B G and Beatty J D 1994 A mouse model for calculating cross-organ beta doses from yttrium-90-labeled immunoconjugates *Cancer* **73** 951–7
Jan S *et al* 2004 GATE: a simulation toolkit for PET and SPECT *Phys. Med. Biol.* **49** 4543–61
Keenan M A, Stabin M G, Segars W P and Fernald M J 2010 RADAR realistic animal model series for dose assessment *J. Nucl. Med.* **51** 471–6
Kolbert K S, Watson T, Matei C, Xu S, Koutcher J A and Sgouros G 2003 Murine *S* factors for liver, spleen, and kidney *J. Nucl. Med.* **44** 784–91 (PMID:12732681)
Kost S D, Dewaraja Y K, Abramson R G and Stabin M G 2015 VIDA: a voxel-based dosimetry method for targeted radionuclide therapy using Geant4 *Cancer Biother. Radiopharm.* **30** 16–26
Kostou T, Papadimitroulas P, Loudos G and Kagadis G C 2016 A preclinical simulated dataset of *S*-values and investigation of the impact of rescaled organ masses using the MOBY phantom *Phys. Med. Biol.* **61** 2333–55
Larsson E, Strand S E, Ljungberg M and Jönsson B A 2007 Mouse *S*-factors based on Monte Carlo simulations in the anatomical realistic Moby phantom for internal dosimetry *Cancer Biother. Radiopharm.* **22** 438–42
Lee M S, Kim J H, Paeng J C, Kang K W, Jeong J M, Lee D S and Lee J S 2018 Whole-body voxel-based personalized dosimetry: the multiple voxel *S*-value approach for heterogeneous media with nonuniform activity distributions *J. Nucl. Med.* **59** 1133–9
Loevinger R, Budinger T F and Watson E E 1988 *MIRD Primer for Absorbed Dose Calculations* (New York: Society of Nuclear Medicine)
Matsumoto M and Nishimura T 1998 Mersenne twister: a 623-dimensionally equidistributed uniform pseudo-random number generator *ACM Trans. Model. Comput. Simul.* **8** 3–30
Mauxion T, Barbet J, Suhard J, Pouget J P, Poirot M and Bardiès M 2013 Improved realism of hybrid mouse models may not be sufficient to generate reference dosimetric data *Med. Phys.* **40** 052501
Muthuswamy M S, Roberson P L and Buchsbaum D J 1998 A mouse bone marrow dosimetry model *J. Nucl. Med.* **39** 1243–7 (PMID:9669402)
Parach A A, Rajabi H and Askari M A 2011 Assessment of MIRD data for internal dosimetry using the GATE Monte Carlo code *Radiat. Environ. Biophys.* **50** 441–50
Perrot Y *et al* 2014 Internal dosimetry through GATE simulations of preclinical radiotherapy using a melanin-targeting ligand *Phys. Med. Biol.* **59** 2183–98
Sarrut D *et al* 2014 A review of the use and potential of the GATE Monte Carlo simulation code for radiation therapy and dosimetry applications *Med. Phys.* **41** 064301
Segars W P, Tsui B M, Frey E C, Johnson G A and Berr S S 2004 Development of a 4D digital mouse phantom for molecular imaging research *Mol. Imaging Biol.* **6** 149–59
Sgouros G, Frey E, Wahl R, He B, Prideaux A and Hobbs R 2008 Three-dimensional imaging-based radiobiological dosimetry *Semin. Nucl. Med.* **38** 321–34
Snyder W S, Fisher H L Jr, Ford M R and Warner G G 1969 Estimates of absorbed fractions for monoenergetic photon sources uniformly distributed in various organs of a heterogeneous phantom *J. Nucl. Med.* **3** 7–52 (PMID:5802194)
Stabin M G and Siegel J A 2003 Physical models and dose factors for use in internal dose assessment *Health Phys.* **85** 294–310
Stabin M G, Peterson T E, Holburn G E and Emmons M A 2006 Voxel-based mouse and rat models for internal dose calculations *J. Nucl. Med.* **47** 655–9 (PMID:16595500)
Stabin M G, Sparks R B and Crowe E 2005 OLINDA/EXM: the second-generation personal computer software for internal dose assessment in nuclear medicine *J. Nucl. Med.* **46** 1023–7 (PMID:15937315)
Taschereau R and Chatziioannou A F 2007 Monte Carlo simulations of absorbed dose in a mouse phantom from 18-fluorine compounds *Med. Phys.* **34** 1026–36
Valentin J 2002 Basic anatomical and physiological data for use in radiological protection: reference values: ICRP Publication 89 *Ann. ICRP* **32** 5–265
Xie T and Zaidi H 2013 Monte Carlo-based evaluation of *S*-values in mouse models for positron-emitting radionuclides *Phys. Med. Biol.* **58** 169–82